



Irregular Implant Design Decreases Periimplant Stress and Strain Under Oblique Loading

Ling He, PhD,* Jiwu Zhang, EB,† Xiucheng Li, PhD,‡ Hongcheng Hu, MD,§ Songhe Lu, MD,§ and Zhihui Tang, MD¶

The success of osseointegrated implants is dependent on the establishment and maintenance of a direct structural and functional link between the surface of the load carrying the implant and the surrounding bone.¹

Crestal bone loss is the most common cause of failure of implants in which osseointegration has been achieved.² In the literature, crestal bone loss has primarily been attributed to 3 factors; plaque-induced periimplantitis which is plaque-induced inflammation in the periimplant tissues with subsequent bone loss^{3,4}; and occlusal overload in which excessive loads applied to the implant may cause pathological stresses and strains in the crestal bone stimulating resorption.^{5–9}

Carter et al found that bone has an extremely poor fatigue strength.¹⁰ It

Objectives: To investigate whether a different implant geometry with the same potential contact surface area (PCSA) affects the principal stress and strains in bone.

Material and Methods: Three-dimensional finite-element models were created with a single endosseous implant embedded in bone. The irregular (IR) dental root-analog implant and regular (R) cylindrical implant with the same PCSA 350 mm² were modeled, keeping the size of the thinnest implant wall 0.8 mm, and the thinnest bone wall 1 mm. The regular or irregular abutments were either 4.5 mm lower than the platform of the implants or 5 mm higher than the platform of the implants, both with the taper 1.44°. A 100 N vertical or 100 N vertical/50 N horizontal occlusal loading was applied. The biomechanical behaviors of periimplant bone were recorded.

Results: The IR implant design experienced lower periimplant stress and strain under oblique loading than that of R implant design. In the IR implant design, comparable stress in bone, implant, and abutment were found under 100 N vertical loading or 100 N vertical/50 N horizontal loading. In the R implant design, much higher stress in bone, implant, and abutment were found under 100 N vertical/50 N horizontal loading than that under 100 N vertical loading.

Conclusion: Irregular dental root-analog implant is a biomechanically favorable design principle for decreasing periimplant stress and strain under oblique loading. (Implant Dent 2017;26:744–750)
Key Words: regular implant, root-analog implant, three-dimensional finite element analysis, horizontal resistance

*Research Assistant, Department of The Second Dental Center, Peking University School and Hospital of Stomatology, Beijing, People's Republic of China.

†Postgraduate, Department of School of Mathematics and Physical, University of Science and Technology Beijing, Beijing, People's Republic of China.

‡Research Assistant, Department of School of Mathematics and Physical, University of Science and Technology Beijing, Beijing, People's Republic of China.

§Attending Doctor, Department of The Second Dental Center, Peking University School and Hospital of Stomatology, Beijing, People's Republic of China.

¶Professor, Department of The Second Dental Center, Peking University School and Hospital of Stomatology, Beijing, People's Republic of China.

Reprint requests and correspondence to: Zhihui Tang, MD, Department of The Second Dental Center, Peking University School and Hospital of Stomatology, No. 66 anliu, Chaoyang District, Beijing 100101, People's Republic of China, Phone: +86 10 82196237, Fax: +86 10 64907970, E-mail: tang_zhihui@live.cn

ISSN 1056-6163/17/02605-744

Implant Dentistry

Volume 26 • Number 5

Copyright © 2017 Wolters Kluwer Health, Inc. All rights reserved.

DOI: 10.1097/ID.0000000000000662

has been suggested that microdamage occurring on a daily basis is a bone maintenance stimulus.¹¹ “Stress fracture” of bone is believed to result from accumulation and coalescence of microdamage occurring when bone remodeling is insufficient to mend the microdamage as it is formed.¹² Hoshaw et al inserted Brånemark implants into adult canine tibiae.⁶ After a healing time of 1 year, the test implants were loaded in axial tension for 500 cycles/d for 5 consecutive days. A net bone

loss was found around the neck of the loaded implants. A finite element analysis showed high strains in this region. This indicated that the bone loss was the result of bone modeling and remodeling secondary to bone microdamage. In light of this finding, it was suggested that a dental implant should be designed such that the peak bone stresses resulting from the loads on the implant are minimized. Thus, an even loading of the available bone is achieved.

In clinical situations, horizontal forces are present, and the magnitude of the force is related to cusp inclination and width of the occlusal table.¹³ For regular and symmetric implants (tapered or cylindrical), the recorded crestal shear strains are proportionally related to the applied loads, larger loads involve higher strains.¹⁴

To avoid excessive stresses in the marginal bone, Mailath et al recommended a smooth endosseous implant neck allowing sliding motion between the implant and bone, to the effect that the marginal bone resists horizontal load components, whereas vertical load components are resisted by the underlying bone.¹⁵ The rationale for this recommendation was that the peak stresses caused by horizontal load components should be spatially separated from the peak stresses caused by vertical load components. However, in a finite element study of an axially loaded dental implant, Hansson obtained a considerably greater peak interfacial shear stress for a low bone attachment level than for a high attachment level.¹⁶ In all calculation examples, the peak stress arose at the level at which the implant started to be retained in the bone. The rationale for using this smooth endosseous implant neck was to avoid bone resorption caused by excessive stresses. However, the results of a number of animal studies have indicated that an endosseous neck devoid of retention elements,^{5,17–23} far from impeding marginal bone resorption, in fact promotes it.^{16,24} It has been suggested that this bone loss is a consequence of insufficient mechanical stimulation of the marginal bone.^{16,18,24}

The more apical location of the peak interface shear stress suggests that the conical implant-abutment interface is a solution to the problem formulated by Mailath et al¹⁵; to spatially separate the peak bone stresses caused by horizontal load components from the peak bone stresses caused by vertical load components.²⁵ Bone stresses are affected by the wall thickness of the implant and by the modulus of elasticity of the implant material.²⁶ Abutment should be designed with a conical interface, such that the peak bone-implant

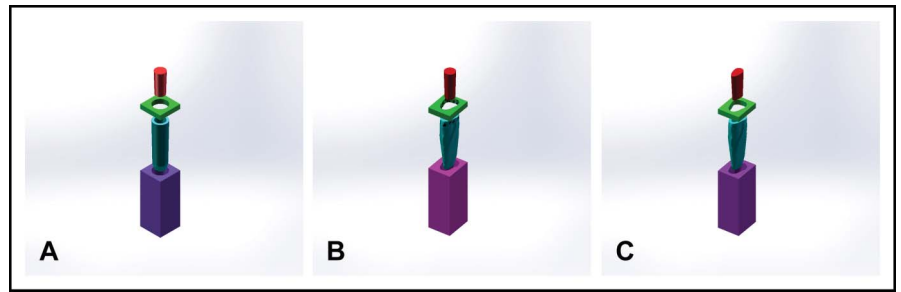


Fig. 1. Three 3D finite element models of the cancellous bone (purple), implant (blue), cortical bone (green), and abutments (red). **A**, represents model A: regular (R) abutment match regular (R) implant in the bone; **B**, represents model B: regular (R) abutment match irregular (IR) implant in the bone; and **C**, represents model C: irregular (IR) abutment match irregular (IR) implant in the bone.

Table 1. Total Number of Elements and Nodes

	Elements	Nodes
Model A	27,383	38,024
Model B	1,116,630	189,390
Model C	1,120,111	190,064

The models were meshed with 3D 4-node tetrahedron elements. The total numbers of elements and nodes are listed above.

interface shear stress has a more apical location.²⁵

Potential contact surface area (PCSA) is the implant surface area which potentially contacts bone, calculated according to the official data of implant companies. PCSA is a reliable mean that accurately represents implant dimensions and may replace length and diameter.²⁷ PCSA is an important index when R and irregular (IR) implants were designed and compared.

One aim of this study was to investigate whether a different implant geometry with the same PCSA in a finite element model affects the principal strains in bone, especially in areas where remodeling and/or resorption is known to occur, such as in the crestal bone region. A second aim of this study was to investigate whether a different abutment geometry with the same thinnest implant wall thicknesses

affects the interface stresses around the abutment.

MATERIALS AND METHODS

Model Design

To obtain the geometry of a patient's canine, a computed tomography (CT) examination was carried out on a volunteer, with approval from the Ethical Committee of the Peking University School of Stomatology (PKUSSIRB-201522061). Her canine was scanned. The CT examination files were then imported into Ansys 15.0 (Ansys Corporation). The irregular (IR) dental root-analog implant was chosen for this biomechanical analysis. The PCSA of the IR implant was calculated to be 350 mm². With the same PCSA, regular (R) cylindrical implant was modeled. The 3-dimensional geometries of the implants and abutments and bone were modeled in SolidWorks 2008 (SolidWorks Corporation, Velizy-Villacoublay, France).

Three 3D finite element analysis (FEA) models, irregular (IR) oval cross-section abutment, and regular (R) circular cross-section abutment were designed (Fig. 1), both keeping the size of the thinnest implant wall

Table 2. Material Properties

	Young Modulus (MPa)	Poisson Ratio	Reference
Ti-6Al-4V	103,400	0.35	Sertgöz and Güvener ²⁸
Cortical bone	13,700	0.3	Barbier et al ²⁹
Cancellous bone	1370	0.3	Barbier et al ²⁹

The abutments and root-analog implant (RAI) were made of Ti6Al4V titanium alloy. The material properties of the cortical and cancellous bone, abutments and implants were determined from values obtained from the literature. All materials were assumed to be isotropic, homogeneous and linearly elastic.

Table 3. Implant and Abutment Design of Model

	Model A	Model B	Model C
Implant	Regular (R)	Regular (R)	Irregular (IR)
Abutment	Regular (R)	Irregular (IR)	Irregular (IR)

Three 3D FEA models.

Model A, regular (R) abutment match regular (R) implant in the bone.

Model B, regular (R) abutment match irregular (IR) implant in the bone.

Model C, irregular (IR) abutment match irregular (IR) implant in the bone.

0.8 mm, the thinnest bone wall 1 mm. The abutments were 4.5 mm lower than the platform of the implants, 5 mm higher than the platform of the implants, both with the taper 1.44°. The geometries of the bone and implants and abutments were modeled and then meshed using Ansys 15.0 (Ansys Corporation).

1. Model A, regular (R) abutment match regular (R) implant in the bone.
2. Model B, regular (R) abutment match irregular (IR) implant in the bone.
3. Model C, irregular (IR) abutment match irregular (IR) implant in the bone.

The models were meshed with 3D 4-node tetrahedron elements. The total numbers of elements and nodes are listed in Table 1.

Material Properties

The bone was composed of a 2-mm constant cortical bone layer around a cancellous bone core. The abutments

and RAI were made of Ti6Al4V titanium alloy. The material properties of the cortical and cancellous bone, abutments and implants were determined from values obtained from the literature (Table 2). All materials were assumed to be isotropic, homogeneous, and linearly elastic.

Contact Management and Loading Conditions

The base of the block was fixed to prevent movements in all directions (x, y, z). It was assumed that a perfect contact for all the interfaces by assigning “bonded” contact type between the implant-bone and abutment-implant surfaces. The bonded contact type is assigned when a perfect union between surfaces is desired, preventing the slip

of 1 over the other or the separation of both. There was no surface penetration for the contacts.

Implants were considered totally osseointegrated. Abutments were considered tightly touched. Therefore, a mechanically perfect interface was presumed to exist between the implant and bone, and the abutment and implant.

The models were constrained at the nodes on the mesial and distal bone in all degrees of freedom. Three types of loads were applied to the abutment in each model to simulate functional loading, namely 100 N vertical load I (V), 100 N vertical/50 N palatal load (VP), 100 N vertical/50 N labial load (VL), and 100 N vertical/50 N mesial load (VM). To facilitate discussion, the 3 loading conditions have been abbreviated as V, VP, VL, and VM for 1 vertical load and 3 vertical/horizontal loads (Table 3).

RESULTS

Table 4 shows the von Mises strain values in the periimplant cortical bone.

Table 5. Maximum von Mises Strains in Periimplant Cortical Bone Under 3 Loading Conditions (MPa)

Loading Condition	Model A	Model B	Model C
V	0.22135	3.84334	3.27247
VP	6.27861	3.84387	3.27247
VL	6.27861	3.85294	3.27247
VM	6.27861	3.80922	3.22995

Maximum von Mises stresses in periimplant cortical bone under 3 loading conditions (MPa).

Loading condition: 100 N vertical load I (V), 100 N vertical/50 N palatal load (VP), 100 N vertical/50 N labial load (VL) and 100 N vertical/50 N mesial load (VM). Palatal load, labial load, mesial load were horizontal load.

Model A, regular (R) abutment match regular (R) implant in the bone.

Model B, regular (R) abutment match irregular (IR) implant in the bone.

Model C, irregular (IR) abutment match irregular (IR) implant in the bone.

In irregular implant design, stress in bone experienced no increase when extra horizontal loading was added.

In irregular implant design, with regular or irregular abutment, stress in bone both experienced no increase.

In regular implant design, stress in bone markedly increased when extra horizontal loading was added.

Table 4. Maximum von Mises Strains in Periimplant Cortical Bone Under 3 Loading Conditions ($\mu\epsilon$)

Loading Condition	Model A	Model B	Model C
V	16.2	283	244
VP	459	283	244
VL	459	283	244
VM	459	280	240

Maximum von Mises strains in periimplant cortical bone under 3 loading conditions ($\mu\epsilon$).

Loading condition: 100 N vertical load I (V), 100 N vertical/50 N palatal load (VP), 100 N vertical/50 N labial load (VL) and 100 N vertical/50 N mesial load (VM). Palatal load, labial load, mesial load were horizontal load.

Model A, regular (R) abutment match regular (R) implant in the bone.

Model B, regular (R) abutment match irregular (IR) implant in the bone.

Model C, irregular (IR) abutment match irregular (IR) implant in the bone.

Periimplant strains are physiologic on the entire crestal surface (not exceed 2,500 $\mu\epsilon$).

Table 6. Maximum von Mises Strains in Implant Cortical Bone Under 3 Loading Conditions (MPa)

Loading Condition	Model A	Model B	Model C
V	5.57179	19.3398	14.712
VP	47.2458	19.3249	16.6364
VL	47.2458	19.3605	16.6364
VM	47.2458	19.3239	14.8014

Maximum von Mises stresses in periimplant cortical bone under 3 loading conditions (MPa).

Loading condition: 100 N vertical load I (V), 100 N vertical/50 N palatal load (VP), 100 N vertical/50 N labial load (VL) and 100 N vertical/50 N mesial load (VM). Palatal load, labial load, mesial load were horizontal load.

Model A, regular (R) abutment match regular (R) implant in the bone.

Model B, regular (R) abutment match irregular (IR) implant in the bone.

Model C, irregular (IR) abutment match irregular (IR) implant in the bone.

In irregular implant design, stress in implant experienced no increase when extra horizontal loading was added.

In irregular implant design, with regular or irregular abutment, stress in implant both experienced no increase.

In regular implant design, stress in implant markedly increased when extra horizontal loading was added.

Table 7. Maximum von Mises Strains in Abutment Under 3 Loading Conditions (MPa)

Loading Condition	Model A	Model B	Model C
V	8.1666	27.7487	22.3037
VP	40.8192	18.9385	14.579
VL	40.8192	18.8232	14.579
VM	40.8192	20.7076	22.459

Maximum von Mises stresses in periimplant cortical bone under 3 loading conditions (MPa).

Loading condition: 100 N vertical load I (V), 100 N vertical/50 N palatal load (VP), 100 N vertical/50 N labial load (VL), and 100 N vertical/50 N mesial load (VM). Palatal load, labial load, and mesial load were horizontal load.

Model A, regular (R) abutment match regular (R) implant in the bone.

Model B, regular (R) abutment match irregular (IR) implant in the bone.

Model C, irregular (IR) abutment match irregular (IR) implant in the bone.

In irregular implant design, stress in abutment experienced no increase when extra horizontal loading was added.

In irregular implant design, with regular or irregular abutment, stress in abutment both experienced no increase.

In regular implant design, stress in abutment markedly increased when extra horizontal loading was added.

Periimplant strains are physiologic on the entire crestal surface (not exceed 2,500 $\mu\epsilon$).

Tables 5–7 show the von Mises stress values in the periimplant cortical bone, implant, and abutments.

Figure 2, A–C show the stresses that occurred in bone around the regular (R) cylindrical implant and the irregular (IR) dental root-analog implant under 100 N vertical/50 N palatal load. In each figure, the areas that were exposed to

equal von Mises stress are shown in the same color. A color scale is provided for each figure.

Figure 2A shows the stress concentration in the bone surrounding the regular cylindrical implant. The highest stress peaks were concentrated at the neck of the implant, whereas the rest of the periimplant bone seemed to bear lower stress.

Figure 2B shows the stress concentration in the bone surrounding the irregular dental root-analog implant with regular abutment. A certain amount of stress seemed to be well distributed in the bone around the implant, with some concentration at its extreme apical portion. Low stress levels were evenly distributed all around the implant. Stress levels increased slightly toward the neck of the implant.

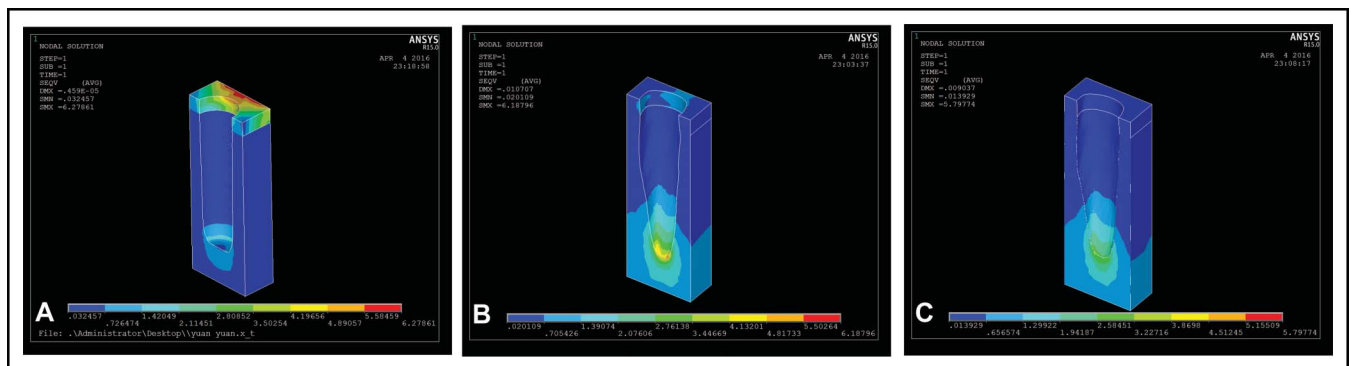


Fig. 2. Stresses at the implant-bone interface in the cortical and cancellous bone. The view is the longitudinal section, but only the part inside the bone box is shown. The implants are not shown. **A**, bone of model A; **(B)** bone of model B; and **(C)** bone of model C. When 100 N vertical/50 N palatal load was imposed, stress distribution in the bone on the labial side is expressed as different colors, blue represents low stress value, and red represents high stress value. **A**, The peak bone stresses were found on the top (6.27 MPa); **(B)** The peak bone stresses were found in the bottom (6.11 MPa); **(C)** The peak bone stresses were found in the bottom (5.79 MPa).

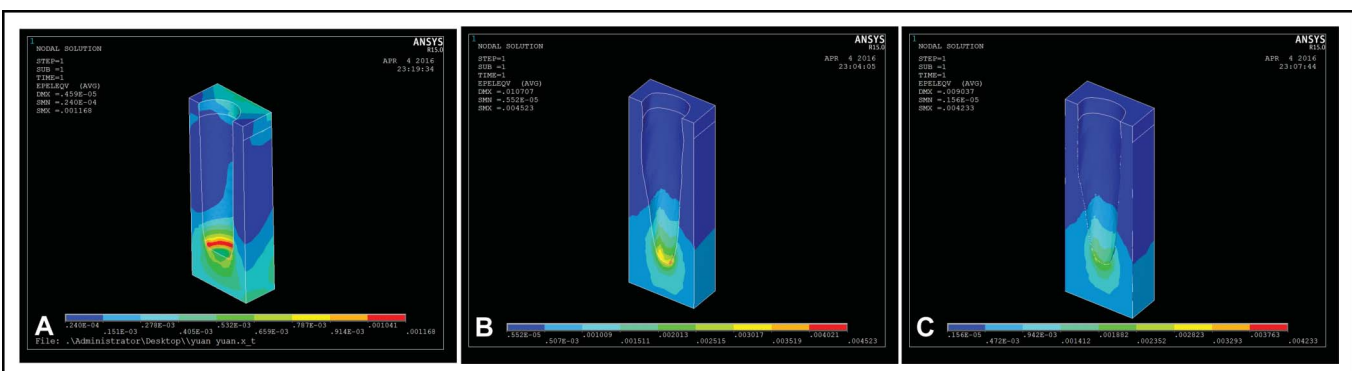


Fig. 3. Strains at the implant-bone interface in the cortical and cancellous bone. The view is the longitudinal section, but only the part inside the bone box is shown. The implants are not shown. **A**, bone of model A; **(B)** bone of model B; and **(C)** bone of model C. When 100 N vertical/50 N palatal load was imposed, strains distribution in the bone on the labial side is expressed as different colors, blue represents low stress value, and red represents high stress value. **A**, The peak bone stresses were found on the top; **(B)** The peak bone stresses were found in the bottom; **(C)** The peak bone stresses were found in the bottom.

Figure 2C shows the stress concentration in the bone surrounding the irregular dental root-analog implant with irregular abutment. Stress seemed to be well distributed in the bone around the implant, with some concentration at its extreme apical portion. Low stress levels were evenly distributed all around the implant. Stress levels increased slightly toward the neck of the implant.

Figure 3, A–C show the strains that occurred in the bone around the regular (R) cylindrical implant and the irregular (IR) dental root-analog implant under 100 N vertical/50 N palatal load. In each figure, the areas that were exposed to equal von Mises strains are shown in the same color. A color scale is provided for each figure. Maximum von Mises strains are all in the cancellous bone region.

DISCUSSION

The results of finite element analysis of a problem like this should be interpreted with some care. The models were axisymmetric; in reality, the problem is 3 dimensional. However, the capacity of modern computers is far from sufficient to solve a realistic 3-dimensional model with a mesh of similar density. The bone was assumed to be linearly elastic; in reality, it is to some extent viscoelastic.³⁰ However, the greatest bone stresses of a regular implant arose close to the implant surface where the remodeling rate is high.³¹ The bone was assumed to be homogenous; in reality, it always contains voids. It was assumed that the interface was frictionless and did not resist any tensile stress, which are also idealistic assumptions. If the purpose had been to find the true bone stresses in a clinical situation, the model would have been inadequate. However, the aim was to study the relative merits of different designs and it is a general experience that rather simple models can give valid results in such cases.³² Thus, the absolute values of the different stresses obtained in this study are of minor interest. What are of interest are the relative values of the different stresses for the different implant designs. It is suggested that the implant

design that gives the best result with a cortical thickness of 2.8 mm would also give the best result with a cortical thickness of 1 mm (the stresses would be much higher). The results of finite element analysis to some extent depend on the size of the elements. If the purpose is to obtain accurate values for the stresses, the element mesh should be refined at locations with large stress gradients. However, the purpose of this study was to compare the stresses and strains in the crestal bone region for different implant designs. In such a situation, it is sufficient if the element mesh is identical in the crestal bone region for the different designs. The models fulfilled these requirements.

To analyze the force transfer characteristics, the implant-abutment complex was embedded in a homogeneous structure, a “bone block,” which was assigned Young modulus and Poisson ratio similar to that of the cancellous bone. This was undertaken to eliminate the effects of variations in bone structure, such as bone density and cortical bone thickness.

In clinical situations, horizontal forces are present, and the magnitude of the force is related to cusp inclination and width of the occlusal table.¹³ For regular and symmetric implants (tapered or cylindrical), the recorded crestal shear strains are proportionally related to the applied loads; larger loads involve higher strains.¹⁴

Potential contact surface area (PCSA) is the implant surface area which potentially contacts bone, and is a reliable means that accurately represents implant dimensions and may replace length and diameter.²⁷ PCSA is an important index when comparing regular-shaped implant and irregular-shaped implant.

In this study, regular (R) cylindrical implant and irregular (IR) dental root-analog implant with the same PCSA 350 mm² were modeled. Regular (R) circular cross-section abutment was designed for the R implant. Regular (R) circular cross-section abutment and irregular (IR) oval cross-section abutment were designed for the IR implant. The least thickness of the alloy surrounding the abutment was 0.8 mm.

It was found that with the same PCSA, irregular (IR) dental root-analog implant effectively resists horizontal load, regardless of the regular or irregular abutment design. Bone and implant experienced almost equal von Mises stress value under 100 N vertical load and 100 N vertical/50 N horizontal load. The crestal strains were also equal, not proportionally related to the applied loads. However, when 100 N vertical/50 N horizontal load was imposed, the stress in bone, implant, and abutment experience a substantial increase in regular (R) cylindrical implant design.

Other studies showed that bone stresses are affected by the design of implant-abutment interface, wall thickness of the implant, diameter of implant, and crestal bone thickness.

The problem formulated by Mailath et al (1989) to obtain the highest bone stresses resulting from axial load components spatially separated from those resulting from horizontal load components can be solved by a proper design of the implant-abutment interface.¹⁵ By means of a conical implant-abutment interface at the level of the marginal bone, conical implant-abutment interface at the level of the marginal bone, is a biomechanically favorable design principle.²⁵ This confirms the finding in other studies that, in general, the peak bone stresses resulting from axial loads arise where the implant starts to become attached to the bone.^{15,16}

In a clinical study, at the baseline the average marginal bone level was 0.47 mm below the upper edge of the implant. Five years later, the average marginal bone level had moved 0.07 mm more coronally. A high and stable marginal bone level for this implant has also been observed in other studies.^{33–35} This might be taken as a clinical support for the finding that a conical implant-abutment interface at the level of the marginal bone, in combination with retention elements at the implant neck, is a biomechanically favorable design principle.³⁶

An increase in wall thickness and an increase in the modulus of elasticity result in an increased axial stiffness of the implant. An increase in wall thickness and an increase in the modulus of

elasticity will bring about an increase in the implant ring stiffness. An increased ring stiffness implies increased resistance in the horizontal direction. The bone stresses are affected by the wall thickness of the implant and by the modulus of elasticity of the implant material.²⁵

Increasing implant diameter resulted in as much as a 3.5-fold reduction of crestal strain, which agrees with other finite element (FE) investigations.³⁷⁻³⁹ The effect was greater for short and tapered implants. Several clinical studies reported higher survival rates and reduced crestal bone loss (mean values ranged between 0.05 and 0.8 mm) for wide-diameter implants.⁴⁰⁻⁴²

Increasing length caused as much as 1.65-fold reduction, whereas the taper increased crestal strain, especially in narrow and short implants, where it increased 1.65 fold. The influence of implant diameter on crestal bone strains dominates over the effect of the implant's length and taper. Diameter, length, and taper have to be considered together because of their interactive effects on crestal bone strain.¹⁴ Crestal bone thickness can influence the crestal strains as shown in previous studies.^{43,44}

In this study, irregular (IR) dental root-analog implant could better resist horizontal load than that of regular (R) cylindrical implant, which could be explained as follows: (1) IR implant simulated natural tooth "asymmetric" geometry, which possess anti-rotation ability when horizontal load was imposed; (2) IR implant simulated natural tooth, with larger sectional area at implant neck. At the level of the marginal bone, sectional area of the IR implant is larger than that of the R implant.

The finding in this study confirm the finding in other clinical studies that, with perfect congruence between implant and extraction socket, the custom-made root-analog implant showed a perfect functional and esthetic integration after 1 year of follow-up.^{45,46}

CONCLUSION

Within the limitations of this *in vitro* study, the following conclusions can be drawn:

1. The maximum von Mises strain values in periimplant bone were within physiological limits in irregular implant and regular implant models.
2. Irregular implant design could resist horizontal load.
3. Regular implant design could not resist horizontal load.
4. Irregular dental root-analog implant is a biomechanically favorable design principle for decreasing periimplant stress and strain under oblique loading.

DISCLOSURE

The authors claim to have no financial interest, either directly or indirectly, in the products or information listed in the article.

APPROVAL

Approval from the ethical committee of Peking University School of Stomatology (PKUSSIRB-201522061).

ROLES/CONTRIBUTIONS BY AUTHORS

L. He provided the idea, did research, data analysis, and wrote the manuscript. J. Zhang designed the FEA model and did research. X. Li designed the FEA model and did research. H. Hu obtained the geometry of tooth from CT examination files. S. Lu obtained the geometry of tooth from CT examination files. Z. Tang provided the fund and instructed the research.

ACKNOWLEDGMENTS

Supported by The National Key Research and Development Program of China (2016YFB1101200).

REFERENCES

1. Brånemark PI, Zarb GA, Albrektsson T, eds. *Tissue-Integrated Prostheses: Osseointegration in Clinical Dentistry*. Vol 77. Chicago, IL: Quintessence Publ; 1985:496-497.

2. Albrektsson T, Zarb G, Worthington P, et al. The long term efficiency of currently used dental implants: A review proposed criteria success. *Int J Oral Maxillofac Implants*. 1986;1:11-25.

3. Albrektsson T, Isidoi F. Consensus report of session IV (implant dentistry). In: Lang NP, Karring T, eds. *Proceedings of the 1st European Workshop on Periodontology*. Chicago, IL: Quintessence; 1994:365-369.

4. Callan DP, O'Mahony A, Cobb CM. Loss of crestal bone around dental implants: A retrospective study. *Implant Dent*. 1998;7:258-265.

5. Quirynen M, Naert I, van Steenberghe D. Fixture design and overload influence marginal bone loss and fixture success in the Brånemark system. *Clin Oral Implant Res*. 1992;3:104-111.

6. Hoshaw SJ, Brunski JB, Cochran GVB. Mechanical loading of Brånemark implants affects interfacial bone modeling and remodeling. *Int J Oral Maxillofac Implants*. 1994;9:345-360.

7. Isidor F. Loss of osseointegration caused by occlusal load of oral implants, a clinical and radiographic study in monkeys. *Clin Oral Implant Res*. 1996;7:143-152.

8. Isidor F. Histological evaluation of peri-implant bone at implants subjected to occlusal overload or plaque accumulation. *Clin Oral Implant Res*. 1997;8:1-9.

9. Brunski JB. In vivo bone response to biomechanical loading at the bone/dental-implant interface. *Adv Dent Res*. 1999;13:99-119.

10. Carter DR, Caler WE, Spengler DM, et al. Fatigue behavior of adult cortical bone: The influence of mean strain and strain range. *Acta Orthop Scand*. 1981;52:481-490.

11. Carter DR, Fyhrie DP, Whalen RT. Trabecular bone density and loading history: Regulation of connective tissue biology by mechanical energy. *J Biomech*. 1987;20:785-794.

12. Prendergast PJ, Huiskes R. Microdamage and osteocyte-lacuna strain in bone: A microstructural finite element analysis. *J Biomech Eng*. 1996;118:240-246.

13. Mornenburg TR, Proschel PA. In vivo forces on implants influenced by occlusal scheme and food consistency. *Int J Prosthodont*. 2003;16:481-486.

14. Petrie CS, Williams JL. Comparative evaluation of implant designs: Influence of diameter, length, and taper on strains in the alveolar crest. A three-dimensional finite-element analysis. *Clin Oral Implant Res*. 2005;16:486-494.

15. Mailath G, Stoiber B, Watzek G, et al. Die Knochenresorption an der Eintrittsstelle osseointegrierter Implantate—ein biomechanisches Phänomen. Eine Finite-Element-Studie [in German]. *Z Stomatol*. 1989;86:207–216.
16. Hansson S. The implant neck: Smooth or provided with retention elements. A biomechanical approach. *Clin Oral Implant Res*. 1999;10:394–405.
17. Pilliar RM, Deporter DA, Watson PA, et al. Dental implant design—effect on bone remodeling. *J Biomed Mater Res*. 1991;25:467–483.
18. Al-Sayyed A, Deporter DA, Pilliar RM, et al. Predictable crestal bone remodelling around two porous-coated titanium alloy dental implant designs. *Clin Oral Implant Res*. 1994;5:131–141.
19. Andersson B. Implants for single-tooth replacement. A clinical and experimental study on the Brånemark ceraone system. *Swed Dent J*. 1995;108(suppl I):1–41.
20. Engquist B, Nilson H, Åstrand P. Single-tooth replacement by osseointegrated Brånemark implants. *Clin Oral Implant Res*. 1995;6:238–245.
21. Hämmerle CH, Brägger U, Bürgin W, et al. The effect of subcrestal placement of the polished surface of ITI implants on marginal soft and hard tissues. *Clin Oral Implant Res*. 1996;7:111–119.
22. Jung YC, Han CH, Lee KW. A 1-year radiographic evaluation of marginal bone around dental implants. *Int J Oral Maxillofac Implants*. 1996;11:811–818.
23. Malevez C, Hermans M, Daelemans P. Marginal bone levels at Brånemark system implants used for single tooth restorations. The influence of implant design and anatomical region. *Clin Oral Implant Res*. 1996;7:162–169.
24. Wiskott HW, Belser UC. Lack of integration of smooth titanium surfaces: A working hypothesis based on strains generated in the surrounding bone. *Clin Oral Implant Res*. 1999;10:429–444.
25. Hansson S. Implant–abutment interface: Biomechanical study of flat top versus conical. *Clin Implant Dentistry Relat Res*. 2000;2:33–41.
26. Hansson SA. Conical implant–abutment interface at the level of the marginal bone improves the distribution of stresses in the supporting bone. *Clin Oral Implant Res*. 2003;14:286–293.
27. Schwartz-Arad D, Gulayev N, Chaushu G. Immediate versus non-immediate implantation for full-arch fixed reconstruction following extraction of all residual teeth: A retrospective comparative study. *J Periodontol*. 2000;71:923–928.
28. Sertgöz A, Güvener S. Finite element analysis of the effect of cantilever and implant length on stress distribution in an implant-supported prosthesis. *J Prosthet Dent*. 1996;76:165–169.
29. Barbier L, Vander Sloten J, Krzesinski G, et al. Finite element analysis of non-axial versus axial loading of oral implants in the mandible of the dog. *J Oral Rehabil*. 1998;25:847–858.
30. Katz JL. Hard tissue as a composite material. 1. Bounds on the elastic behavior. *J Biomech*. 1971;4:455–473.
31. Roberts WE, Marshall KJ, Mozsay PG. Rigid endosseous implant used as anchorage to protract molars and close an atrophic extraction site. *Angle Orthod*. 1990;60:135–152.
32. Meijer HJA, Starmans FJM, Bosman F, et al. A comparison of three finite element models of an edentulous mandible provided with implants. *J Oral Rehabil*. 1993;20:147–157.
33. Nordin T, Jönsson G, Nelvig P, et al. The use of a conical fixture design for fixed partial prostheses. A preliminary report. *Clin Oral Implant Res*. 1998;9:343–347.
34. Norton M. Marginal bone levels at single tooth implants with a conical fixture design. The influence of surface macro- and microstructure. *Clin Oral Implant Res*. 1998;9:91–99.
35. Puchades-Roman L, Palmer RM, Palmer PJ, et al. A clinical, radiographic, and microbiologic comparison of astra tech and Brånemark single tooth implants. *Clin Implant Dent Relat Res*. 2000;2:78–84.
36. Palmer RM, Palmer PJ, Smith BJ. A 5-year prospective study of astra single tooth implants. *Clin Oral Implant Res*. 2000;11:179–182.
37. Matsushita Y, Kitoh M, Mizuta K, et al. Two-dimensional FEM analysis of hydroxyapatite implants: Diameter effects on stress distribution. *J Oral Implantol*. 1990;16:6–11.
38. Holmgren EP, Seckinger RJ, Kilgren LM, et al. Evaluating parameters of osseointegrated dental implants using finite element analysis—a two-dimensional comparative study examining the effects of implant diameter, implant shape, and load direction. *J Oral Implantol*. 1998;24:80–88.
39. Tada S, Stegaroiu R, Kitamura E, et al. Influence of implant design and bone quality on stress/strain distribution in bone around implants: A 3-dimensional finite element analysis. *Int J Oral Maxillofac Implants*. 2003;18:357–368.
40. Ivanoff CJ, Grondahl K, Sennerby L, et al. Influence of variations in implants diameters: A 3- to 5-year retrospective clinical report. *Int J Oral Maxillofac Implants*. 1999;14:173–180.
41. Renouard F, Arnoux JP, Sarment DP. Five-mm-diameter implants without a smooth surface collar: Report on 98 consecutive placements. *Int J Oral Maxillofac Implants*. 1999;14:101–107.
42. Winkler S, Morris HF, Ochi S. Implant survival to 36 months as related to length and diameter. *Ann Periodontol*. 2000;5:22–31.
43. Holmes DC, Loftus JT. Influence of bone quality on stress distribution for endosseous implants. *J Oral Implantol*. 1997;23:104–111.
44. Petrie CS, Williams JL. Shape optimization of dental implant designs under oblique loading using the p-version finite element method. *J Mech Med Biol*. 2002;2:339–345.
45. Figliuzzi M, Mangano F, Mangano C. A novel root analogue dental implant using CT scan and CAD/CAM: Selective laser melting technology. *Int J Oral Maxillofac Surg*. 2012;41:858–862.
46. Mangano FG, Cirotti B, Sammons RL, et al. Custom-made, root-analogue direct laser metal forming implant: A case report. *Lasers Med Sci*. 2012;27:1241–1245.